Multi-qubit parity measurement in circuit quantum electrodynamics

2013 New J. Phys. 15 075001

(http://iopscience.iop.org/1367-2630/15/7/075001)

New Journal of Physics
The open access journal for physics

Multi-qubit parity measurement in circuit quantum electrodynamics

David P DiVincenzo[1,2,3] **and Firat Solgun**[2,3]

[1] Peter Grünberg Institute: Theoretical Nanoelectronics, Research Center Jülich, Germany
[2] Institute for Quantum Information, RWTH Aachen, Germany
[3] Jülich-Aachen Research Alliance (JARA), Fundamentals of Future Information Technologies, Germany
E-mail: d.divincenzo@fz-juelich.de and firat.solgun@gmail.com

New Journal of Physics **15** (2013) 075001 (18pp)
Received 16 November 2012
Published 2 July 2013
Online at http://www.njp.org/
doi:10.1088/1367-2630/15/7/075001

Abstract. We present a concept for performing direct parity measurements on three or more qubits in microwave structures with superconducting resonators coupled to Josephson-junction qubits. We write the quantum-eraser conditions that must be fulfilled for the parity measurements as requirements for the scattering phase shift of our microwave structure. We show that these conditions can be fulfilled with present-day devices. We present one particular scheme, implemented with two-dimensional cavity techniques, in which each qubit should be coupled equally to two different microwave cavities. The magnitudes of the couplings that are needed are in the range that has been achieved in current experiments. A quantum calculation indicates that the measurement is optimal if the scattering signal can be measured with near single-photon sensitivity. A comparison with an extension of a related proposal from cavity optics is presented. We present a second scheme, for which a scalable implementation of the four-qubit parities of the surface quantum error correction code can be envisioned. It uses three-dimensional cavity structures, using cavity symmetries to achieve the necessary multiple resonant modes within a single resonant structure.

Contents

1. Introduction

The essence of error correcting either quantum or classical information is parity checking. In all practical quantum error correction codes [1], the error-free state is signaled by parities of a selection of subsets of qubits all being 'even'; conversely, the occurrence of 'odd' parities indicates a non-trivial *error syndrome*, with which the particular form of error can be diagnosed. Calculations show that remarkably simple codes are very effective as the substrate of fault tolerant quantum computation; the subsets subjected to parity checks are geometrically local on a two-dimensional (2D) lattice. In addition, the weight of the parity checks is low; for the canonical code of this class, the Kitaev toric code [2], the weights of all checks are four.

It has been standard to assume that a qubit parity should be obtained by computation, in particular by a series of two-qubit quantum logic gates. Thus for the weight-four case, the circuit involves four controlled-NOT gates from each of the four qubits in succession to a fifth, ancilla qubit. The ancilla then holds the value of the parity (or is, perhaps, in an entangled superposition of the two different parity states), so that a measurement of the ancilla reveals (or fixes) this parity. In this paper, we show that, by use of standard microwave scattering techniques, the parity of a small subset of qubits may be measured *directly*, without the need of an intermediate calculation requiring a logic circuit. We hope that this will simplify the process of error correction, and improve thereby its error robustness.

We first discuss some features of the parity determination that are of a particularly quantum-mechanical character. Firstly, it cannot be trivially assumed that after a quantum measurement records some value, the state of the quantum object necessarily still has that value. For example, if a polarization-sensitive photodetector 'clicks' to indicate the polarization of the photon, the photon possessing that polarization will have vanished. In quantum mechanics there is a name for measurements for which the quantum object remains in the state that is recorded: these are called *quantum non-demolition* (QND) measurements. Fortunately, there are many implementations of QND-type measurements, and the types of scattering measurements proposed here will have the QND character.

Secondly, there is a choice of basis involved in defining parity. Thus, while in the classical basis (called the 'Z basis' [1]) we would call 0000, 0011, 0110, etc the even parity states, it is possible to take the basis of the qubit to be, for example $|+\rangle = (|0\rangle + |1\rangle)/\sqrt{2}$ and $|-\rangle = (|0\rangle - |1\rangle)/\sqrt{2}$. In this 'X basis', the even parity states are $++++$, $++--$, $+--+$, etc. In fact, both the X- and Z-type parity checks are needed in quantum error correction. We will introduce a parity measurement for just one basis, understanding that it is possible to apply one-qubit gates

to rotate the qubits so that the parity detection is either of X- or of Z-type. In the superconducting qubit systems that we discuss, these one-qubit rotations can be performed very accurately and quickly.

Thirdly, it is crucial that the parity measurements reveal *only* the parity, and nothing more. For example, the states 0000 and 0011 should both give parity 'even', and should be seen as identical in the measurement process. This concept has no meaning in the classical setting, where 0000 and 0011 represent objectively different states. Quantum mechanics permits a state like $(|0000\rangle + |0011\rangle)/\sqrt{2}$, which does not have a specific, definite bit state, but which nevertheless has a definite parity. In fact, we employ here a strengthening of the idea of QND, which traditionally requires only that a quantum state remains in a certain subspace after measurement. For the measurements that we need, the state is to remain exactly unchanged, and two states with the same parity should reveal nothing of the differences between them.

In quantum physics, this final concept has been given a name, the *quantum eraser* [3]. This name refers to the fact that typically in the course of the measurement process, information is temporarily imprinted on the measurement probe, which is however erased by the end of the measurement process. In interferometry this information is the *welcher weg* ('which path') information which temporarily exists while a photon is moving through the interferometer. This information is erased by the passage of the photon through the final beam splitter of the interferometer. In the implementation we develop below, the measurement probe will temporarily have 'which bitstring' information, which, by the time the scattering process is complete, will be all erased, except for a single bit of parity information. We will show explicitly two different microwave protocols which will permit this *quantum eraser condition* to be satisfied; we will in fact precisely quantify the degree to which this condition is fulfilled.

Discussions of parity measurements are not new to quantum computing theory; it was understood almost from the beginning that two-qubit parity measurement permitted the implementation of standard two-qubit logic gates [4]. A wide variety of two-qubit implementations have been proposed, in electron optics [5], for spin qubits in quantum dots [6] and for charge qubits [7]. The previous discussions of two-qubit parity measurement for atoms in optical cavities [8], and for superconducting qubits [9, 10], will be particularly relevant for this work. Other theoretical work has simulated the details of the parity measurement process [11, 12], and more generally of 'joint measurement', in which other two-qubit operators than the parity are detected. Such joint measurements have been achieved in the area of circuit QED [13–16], the implementation that we discuss here.

In particular, for the application to fault-tolerant error correction [17, 18], it is very important to go beyond two-qubit parity. While quantum error correction codes are known for which two-qubit parity measurements do suffice [19], they are found to have much worse threshold-rate behavior than the Kitaev code [2], which requires four-qubit checks [20]. The Bacon–Shor codes [21] also permit error correction with only two-bit parity checks, and have rather good error correction performance [22], but cannot achieve fault-tolerant operation by only local operations [23]. Many architectural details of a quantum computer employing the surface code have been worked out [24], and the outlook seems quite favorable [20, 25, 26]. Much less is known about the efficacy of three-qubit parity measurements for error correction, although there is a very promising, recent preliminary result [27].

Extending existing two-qubit parity measurements to more than two is not trivial. Classically combining many two-bit parity results to obtain a multi-qubit parity is not permitted, as the overall quantum eraser condition is not satisfied in this case. A real modification of

the measurement protocol or of the coupling structure is necessary. For some other existing schemes [9, 10], we see no reasonable extension to more than two-qubits; in the case of Kerchhoff *et al* [8] such an extension is possible, as we note below. There is another related proposal for a multi-qubit parity measurement in optical systems [28] based on the acquisition of successive small phase shifts by a probe beam; this scheme seems to require some fine tuning, and has no clear extension beyond three qubits. A very recent proposal shows another technique related to the one we present here for extracting multi-qubit parities [29].

We present here a new solution, requiring a specifically designed cavity (or multi-cavity) structure with multiple, closely spaced resonant modes. We first provide a detailed proposal for performing the three-qubit parity measurement, with accurate satisfaction of the quantum eraser condition, in circuit quantum electrodynamics using superconducting qubits. In the current work the preferred type of superconducting qubit is the 'transmon' type [30], although other types would also be possible [31]. We will always require that the couplings between qubits and microwave resonators be in the well-studied 'dispersive regime' [32, 33], in which the qubit transition frequency and the microwave resonant frequency are well separated. In this regime, the qubit gives a state-dependent shift to the resonant frequency of a microwave cavity—one shift for qubit state $|0\rangle$, and a different shift for qubit state $|1\rangle$ (note that states 0 and 1 are at different energies). In this regime, the requirements of the multi-qubit parity measurement reduce to those of a classical microwave design problem.

Our first proposal requires a particular hardware arrangement, involving a capability that has been developed only in the most recent experimental literature [34, 35]. In particular, we require the qubits involved in a three-qubit parity measurement each to have equal dispersive coupling to two different resonant modes. In the first version of our proposal described below, these two different modes are realized as the fundamental modes of two different microwave resonators. Crucial for the proposal is that each resonance should occur at nearly (but not exactly) the same frequency. This near-coincidence allows a scattering phase shift to wind through $2 \times 2\pi$ over a narrow range of frequency. For the four-qubit parity, a winding of 6π is needed, requiring three closely spaced resonant modes to be involved. Our second proposal will deal with this case. We will show that multiple *resonances* need not require multiple *resonators*. This proposal will use the currently popular three-dimensional ('3D') cavity [36], but one having a nearly cubical shape so that the three lowest TE_{101}-type modes [37] are nearly degenerate. We will show a hypothetical scalable implementation of the surface code within this scheme.

2. Results—two-dimensional resonant structure

We will first show that the necessary quantum-erasure function can be realized by the choice of circuit hardware illustrated in figure 1. We will work through and discuss the case of the parity measurement for three qubits; generalizing our construction to more qubits is clear, and will be discussed below. In this construction, we have two resonators (we envision 1/4-wave coplanar waveguide resonators [38], as illustrated schematically); in each we will employ one resonant mode, with creation operators $a^\dagger$ and $b^\dagger$. It would be normal to use the lowest-frequency (fundamental) modes; all other modes are far separated in frequency (the next being at three times the fundamental, in a 1/4-wave structure) and will be ignored. In our scheme, these two fundamental frequencies ω_a and ω_b should be almost, but not exactly, degenerate. The qubit–cavity coupling will be the standard one given by the Jaynes–Cummings model in the dispersive regime [33]. It will be non-standard only in that each qubit will couple

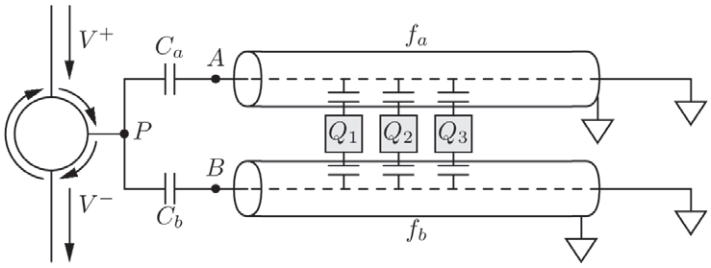

Figure 1. A schematic circuit QED setup for measuring the parity of three qubits. Two transmission-line resonators have slightly different resonant frequencies f_a and f_b. The three qubits $Q_{1,2,3}$ (which could be of the transmon type) each couple equally to the two resonators. The parity information is contained in the phase of the reflection coefficient at point P, which, throughout the action of the circulator, appears as a phase change of the output signal V^- relative to the input tone V^-.

to both resonators, so that each qubit j will have a physical coupling strength $g_{j,a}$ to the a resonator and $g_{j,b}$ to the b resonator. The Hamiltonian of the system of resonators and qubits can be written as [32]

$$H = \left(\omega_a + \sum_{j=1}^{3} \chi_a^j \sigma_z^j\right) a^\dagger a + \left(\omega_b + \sum_{j=1}^{3} \chi_b^j \sigma_z^j\right) b^\dagger b + \frac{1}{2}\sum_{j=1}^{3} \omega_j \sigma_z^j. \tag{2.1}$$

Here ω_j are the qubit frequencies, and the dispersive coupling parameters are $\chi_a^j = g_{j,a}^2/\Delta_{j,a}$ with $\Delta_{j,a} = \omega_j - \omega_a$, and similarly for χ_b^j and $\Delta_{j,b}$. Note that we assume that the system should be engineered so that there is no direct coupling between qubits.

As indicated in figure 1, this resonator/qubit structure is to be coupled capacitively to a scattering probe. Rather than extend our Hamiltonian to include all these other details, we proceed in the following way: since H commutes with each σ_z^j, we can examine the Hamiltonian separately in each of its 2^3 qubit eigensectors; within each of these sectors H describes a harmonic bosonic system, with qubit-dependent resonant-frequency parameters. Thus, the full scattering experiment can be described quite economically using the classical language of impedance and scattering parameters; the conclusions we draw from this classical discussion will have an immediate, standard quantum interpretation in terms of coherent-state propagation.

From ordinary electrical transmission line theory, the impedance between point A in figure 1 and ground is given by

$$Z_A(\omega) = \mathrm{i} Z_0 \tan\left(\frac{\pi}{2}\frac{\omega}{\omega_{r,a}}\right). \tag{2.2}$$

Here $Z_0 = 50\Omega$ is the impedance of the waveguide. The effective resonant frequency ω_r is dependent on the state of the three qubits $|s_1 s_2 s_3\rangle$ according to

$$\omega_{r,a} = \omega_a + \sum_{j=1}^{3} (-1)^{s_j} \chi_a^j. \tag{2.3}$$

This same discussion applies to the qubit-state-dependent impedance $Z_B(\omega)$ of the B resonator. The impedance $Z_P(\omega)$ of the entire structure at point P is then given by ordinary series and

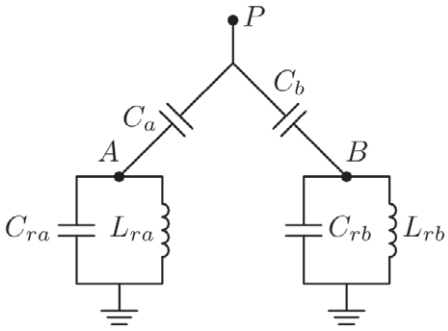

Figure 2. Equivalent circuit for the double-resonator structure [38]; $C_{ra} = \frac{\pi}{4\omega_{r,a}Z_0}$, $L_{ra} = \frac{1}{\omega_{r,a}^2 C_{ra}}$, $C_{rb} = \frac{\pi}{4\omega_{r,b}Z_0}$, $L_{rb} = \frac{1}{\omega_{r,b}^2 C_{rb}}$.

parallel-combination rules. In fact in the frequency range of interest, the response is very well represented by the lumped circuit of figure 2.

The measurable quantity for this structure is the reflection coefficient r at P. This is given by [38]

$$r(\omega) = \frac{V^-(\omega)}{V^+(\omega)} = \frac{Z_P(\omega) - Z_0}{Z_P(\omega) + Z_0}. \tag{2.4}$$

Note that because Z_P is purely imaginary (lossless), $|r| = 1$, so that only the phase of r,

$$\theta(\omega) \equiv \arg r(\omega), \tag{2.5}$$

contains information (which can in fact be measured interferometrically).

Our object is to find a probe frequency ω_p such that the reflected signals for all the even-parity qubit states and all the odd-parity states are indistinguishable, but that the reflection coefficients for the even and odd cases are distinct. This will give us conditions on the reflected phase $\theta_{s_1 s_2 s_3}(\omega_\mathrm{p})$ for the different qubit state settings. A general feature of the θ function will make this possible in our two-resonance setting. If ω passes through a resonance of the system (pole of Z_P), then, while the phase change of the impedance is π, the change of the reflected phase is 2π (cf equations (2.4) and (2.5)). We will arrange that Z_P has two poles within a narrow range of frequency; this means that $\theta(\omega)$ will vary smoothly over 4π in that range. But, from the point of view of a scattered tone, θ and $\theta + 2\pi n$ are indistinguishable. Thus, the $\theta(\omega)$ function varies over a sufficient range that we can satisfy our quantum eraser condition for the parity measurement in the following way:

$$\theta_\mathrm{even} \equiv \theta_{000}(\omega_\mathrm{p}) = \theta_{011}(\omega_\mathrm{p}) + 2\pi, \tag{2.6}$$

$$\theta_\mathrm{odd} \equiv \theta_{111}(\omega_\mathrm{p}) = \theta_{001}(\omega_\mathrm{p}) - 2\pi. \tag{2.7}$$

Since the χ coefficient for all qubits is taken to be equal, the other necessary conditions, $\theta_{011}(\omega_\mathrm{p}) = \theta_{101}(\omega_\mathrm{p}) = \theta_{110}(\omega_\mathrm{p})$ and $\theta_{001}(\omega_\mathrm{p}) = \theta_{010}(\omega_\mathrm{p}) = \theta_{100}(\omega_\mathrm{p})$, are satisfied automatically. It is also necessary that $\theta_\mathrm{even} \neq \theta_\mathrm{odd} \pmod{2\pi}$, with the best case (most distinguishable) being $\Delta\theta \equiv \theta_\mathrm{even} - \theta_\mathrm{odd} = \pi$.

One can show that for any choice of parameters in the two-pole circuit, there exists a probe frequency ω_p and a dispersive shift constant χ such that the parity-measurement conditions (equations (2.6) and (2.7)) are satisfied. However, if the resonant frequencies ω_a and ω_b are

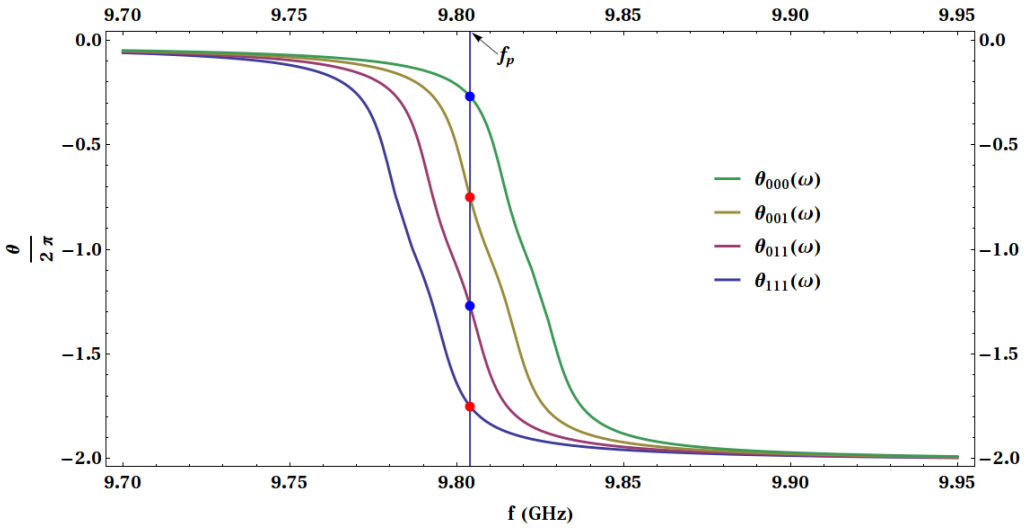

Figure 3. Solution for realistic values $\omega_a = 2\pi\,(9.99\,\text{GHz})$, $\omega_b = 2\pi\,(10.01\,\text{GHz})$, $C_a = C_b = 10\,fF$; with $\omega_\text{p} = 2\pi\,(9.804\,\text{GHz})$, $\chi = 5.77\,\text{MHz}$, giving $\Delta\theta = 172.9°$. Blue points correspond to even states whereas red points correspond to odd states. Vertical blue line shows the probe frequency $f_\text{p} = 9.804\,\text{GHz}$.

far apart compared with the width of the resonances, $\theta_\text{even} - \theta_\text{odd}$ is very small. By placing the resonances close to one another and choosing the capacitance values carefully, a favorable solution can be found. We note that for further optimization of this structure, there would be no difficulty in replacing the simple pair of capacitors $C_{a,b}$ with a capacitance bridge in a wye- or delta-configuration [38].

Figure 3 shows a solution for the case of a realistic set of parameters. The choices are $\omega_a = 2\pi\,(9.99\,\text{GHz})$, $\omega_b = 2\pi\,(10.01\,\text{GHz})$, $C_a = C_b = 10\,fF$; note that realistic values for coupling capacitors are in the $0.5 - 50\,fF$ range (see [39]). Our equations (2.6) and (2.7) are satisfied (after a simple, efficient numerical search) for $\omega_\text{p} = 2\pi\,(9.804\,\text{GHz})$ and $\chi = 5.77\,\text{MHz}$, giving the nearly optimal value $\Delta\theta = 172.9°$. Note that the coupling capacitors will introduce T_1 qubit relaxation, but we can estimate that capacitances on this scale give a cavity loss rate of $\kappa \sim 5\,\text{MHz}$. The Purcell formula for the resulting qubit relaxation time is $T_{1(\text{P})} = \frac{\Delta^2}{\kappa g^2} = \frac{\Delta}{\kappa\chi}$. If we assume $\Delta = 5\,\text{GHz}$, this gives $T_{1(\text{P})} \sim 200\,\mu\text{s}$. Thus, the Purcell mechanism for relaxation will not be a severe limit on the lifetime of the qubits.

We can qualitatively assess the result of applying the measurement tone for a finite length of time. The signal-to-noise ratio for distinguishing even from odd is largely a technical matter involving the noise performance of amplifiers and the effective temperature of filters associated with the resonator-qubit structure. The quantum-erasure property sets a more fundamental limit. If the measurement time is T, the measurement signal will then have a bandwidth $W \sim 1/T$ around the probe frequency ω_p, because the dispersion of the reflection response is different for the different even and odd states (that is, $\frac{\text{d}\theta}{\text{d}\omega}$ is different for the distinct states, see figure 3). Thus we expect that to maintain the quantum-eraser condition, the bandwidth W should be kept to a small fraction of the resonance width, so perhaps $T \sim 10/\chi$. This gives a measurement time $T \sim 2\,\mu\text{s}$. While this is shorter than the expected T_1 in current devices, it would be desirable

to shorten T; we expect that further optimization of the scattering structure could make all the $(\frac{d\theta}{d\omega})_{odd}$ and $(\frac{d\theta}{d\omega})_{even}$ more nearly equal, so that perhaps T could approach $1/\chi$.

A detailed calculation, given in the appendix, confirms these qualitative considerations. This calculation involves a quantum treatment of the input tone V^+, in which it is written as a coherent state [40] $|\alpha\rangle$, pulsed with a Gaussian time profile with characteristic time $T = 1/W$. The pulse has mean photon number $|\alpha|^2$, and therefore energy $\hbar\omega_p|\alpha|^2$. The output tone V^- is also a coherent state $\beta_{\mathbf{s}}$, but dependent on the qubit state $|\mathbf{s}\rangle = |\mathbf{s_1 s_2 s_3}\rangle$. The coherent state amplitude is always unchanged, $|\beta_{\mathbf{s}}| = |\alpha|$, but it is dispersed differently for each state because of the scattering phase shift.

The relevant result from the appendix is

$$\langle\beta_{\mathbf{s}}|\beta_{\mathbf{s}'}\rangle = 1 - \frac{|\alpha|^2 b^2 W^2}{2} + O(|\alpha|^4 b^4 W^4), \quad \text{qubit parities } \mathbf{s} \text{ and } \mathbf{s}' \text{ the same,} \tag{2.8}$$

$$\langle\beta_{\mathbf{s}}|\beta_{\mathbf{s}'}\rangle = \mathrm{e}^{-|\alpha|^2(1-\cos\Delta\theta)}\left(1 + O\left(W\frac{\mathrm{d}\theta}{\mathrm{d}\omega}\right)\right), \quad \text{qubit parities } \mathbf{s} \text{ and } \mathbf{s}' \text{ different.} \tag{2.9}$$

The new parameter b is the first-order difference of phase dispersion

$$b \equiv \theta'_{\mathbf{s}}(\omega_p) - \theta'_{\mathbf{s}'}(\omega_p). \tag{2.10}$$

The quantum-eraser condition requires that the 'same parity' cases be indistinguishable ($\langle\beta_{\mathbf{s}}|\beta_{\mathbf{s}'}\rangle = 1$), and the 'different parity' cases be perfectly distinguishable ($\langle\beta_{\mathbf{s}}|\beta_{\mathbf{s}'}\rangle = 0$). Noting that, on dimensional grounds, $b \sim 1/\chi$, these quantum-erasure conditions are well approximated so long as $T = 1/W > |\alpha|b \sim |\alpha|/\chi$. This confirms the qualitative discussion above, with the additional insight that it is best if the probe is not too strong, i.e. if α is not too large (or course, it should be greater than one to satisfy the 'different parity' condition). If the photon number is taken to be $|\alpha|^2 = 5$, and the pulse duration is $T \approx 1\,\mu$s, the peak pulse power will be about $P = \frac{|\alpha|^2\hbar\omega_p}{T} = -135$ dBm. This is indeed a weak signal, but in the detectable range with the current state of the art [41].

2.1. Comparison with Kerchhoff et al

Before presenting our second proposal, we can compare our concept for three-qubit parity with the three-qubit extension of the two-qubit parity measurement that was recently proposed by Kerchhoff *et al* [8]. They propose sequential scattering from a set of cavities, each coupled to one qubit; the extension of their idea to three qubits, as rendered in plausible microwave components, is shown in figure 4. Note that for n-qubit parity this scheme uses n resonators, while a generalization of our scheme above would use $\lceil (n+1)/2 \rceil$ resonators (see the following section). The Kerchhoff *et al* scheme is certainly elegant, and simpler in that each qubit only needs to couple to a single cavity. The idea is to choose the coupling and the probe tone such that there is a phase difference of π between qubit states 0 and 1; then this network constructs a sum of the phases for each qubit [42].[4] Each cavity should have exactly the same resonant frequency (perhaps by tuning). This scheme is more obviously scalable to more qubits than ours, and it would be possible in this scheme to get rid of the first-order dispersion effects which degrade

[4] We have learned that the method stated here of synthesizing a desired circuit response by cascaded circulators was known a long time ago; it is attributed to Desoer and Belevitch in [42].

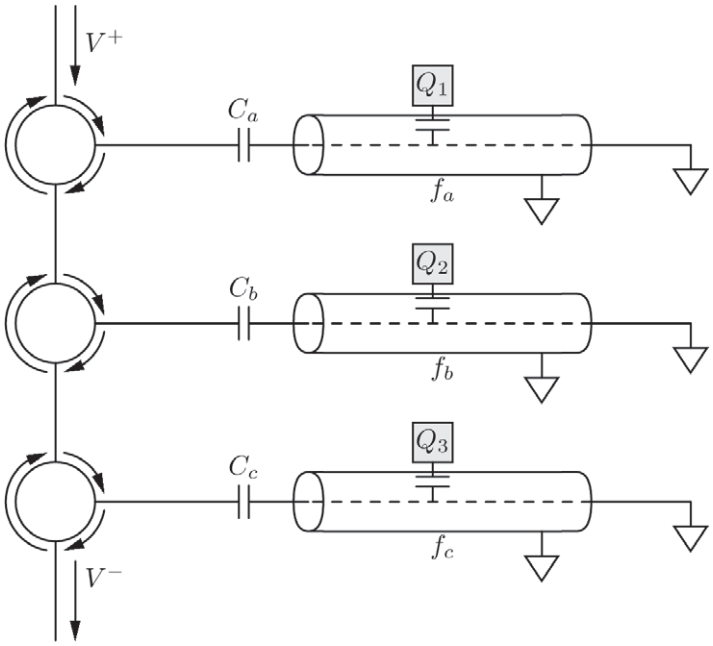

Figure 4. Circuit for three-qubit extension of the scheme proposed as a cavity-optics experiment in [8], as it would be implemented with microwave components in circuit QED.

the quantum-eraser condition, as calculated above. But, as we show in the appendix, the second-order dispersion difference, which would still be present, leads to similar qualitative limits on the measurement time and fidelity. Also, we point out that the quantum-eraser condition would also be degraded by imperfections in the circulators, unlike in our scheme. Given that there presently are no on-chip circulators suitable for qubit experiments (but see progress in [43, 44]), we believe that our scheme is closer to being realized with currently available components.

3. Results—three-dimensional resonant structures

The theoretical generalization of our scheme to the measurement of the arguably more important case of four-qubit parity is straightforward. We require three closely spaced resonances f_a, f_b and f_c, equal coupling χ of each qubit to each of the three resonances, and a network that couples resonators to a single reflected probe. In this case again all measurable quantities will emerge from a single reflected-phase function $\theta_s(\omega)$. Since this function will vary smoothly over 6π, it will be possible to satisfy the three quantum-eraser equations for this case:

$$\theta_{\text{even}} = \theta_{0000}(\omega_p) = \theta_{0011}(\omega_p) + 2\pi = \theta_{1111}(\omega_p) + 4\pi, \tag{3.1}$$

$$\theta_{\text{odd}} = \theta_{0111}(\omega_p) = \theta_{0001}(\omega_p) - 2\pi. \tag{3.2}$$

Tuning the f_i values, χ and ω_p give enough freedom so that these equations should always be solvable. The analogous conditions for n-qubit parity are straightforward to write down; if we use the notation $\theta_{Wt.i}$ to indicate the phase shift if i of the quibits are 1, then the condition is

$$\theta_{Wt.i}(\omega_p) = \theta_{Wt.i+2k}(\omega_p) + 2k\pi. \tag{3.3}$$

Combined with the desire that $\theta_{\mathrm{W}t.0}(\omega_\mathrm{p}) \approx \theta_{\mathrm{W}t.1}(\omega_\mathrm{p}) + \pi$, we see that the θ function should vary by at least πn. For even n this will be accomplished with $n/2+1$ resonances (so that θ winds through phase $\pi(n+2)$), while for odd n, $(n+1)/2$ resonances suffice (θ winds through phase $\pi(n+1)$ in this case). For both even and odd n, the number of resonances required can be written $\lceil (n+1)/2 \rceil$, as stated above.

Returning to the consideration of four-qubit parity, we see that some new hardware elements would be required to achieve this by an extension of the '2D' (coplanar waveguide) scheme above. The requirement that each qubit be equally coupled to each of three different coplanar waveguide (CPW) resonators has not previously been achieved. It seems likely that it is doable with the use of air bridges, which have only recently entered the toolkit of quantum microwave engineering (see [45, 46]). Another possible way to obtain the multiple resonant modes needed for multi-qubit parity measurement would involve the use of multi-conductor CPWs [45], which naturally support modes that are closely spaced in frequency.

But given these difficulties, we explore a second protocol to achieve the implementation of four-qubit parity measurement, involving '3D' superconducting cavities [36]. These high-quality factor rectangular cavities have recently been proven to be excellent implementations of nearly decoherence-free Jaynes–Cummings physics [29]. In these the qubit–cavity coupling is provided by antenna structures extending out from the transmon qubits [36]. Multi-qubit structures [47] have been achieved in this technology, and bridging qubits, antenna-coupled to two different cavities, are now possible [48]. This second protocol illustrates a further fact, which is that *multiple*, closely spaced resonances can be achieved within a *single* resonant structure.

Figure 5 illustrates the concept of this second protocol, also showing how it could be extended to be part of a scalable implementation of the surface code architecture [24, 49]. The key modification in this structure is that the 3D cavities, rather than having a large aspect ratio in which $w \gg l \gg h$ ($w =$ width, $l =$ length, $h =$ height), should be nearly, but not exactly, cubical. Thus, the three lowest resonant modes would be nearly degenerate in frequency, since their wavelengths will be set by π/w, π/l and π/h. (Be warned that the traditional labels for these modes are TE_{101}, TE_{011} and TM_{110} [37].) Each cavity is coupled, via antenna structures, to four qubits, two on the front surface in figure 5 and two on the back (not shown). Each antenna runs along the body diagonal (i.e. $\langle 111 \rangle$ axis) of the cubical cavity; with this geometry the coupling is equal to each of the three eigenmodes, whose modal electric field patterns point straight along one of the three coordinate axes.

Unlike for our first ('2D') proposal, we will not provide calculations of the performance of the structure of figure 5. While the structure of figure 1 can be analyzed using elementary transmission line theory and a few component parameter values whose ranges are well understood, the system of figure 5 is a complex, 3D structure whose electromagnetic response can only be obtained reliably by detailed calculations that are beyond the scope of this paper. It is encouraging that progress is being made in the detailed modeling of couplings in such a 3D geometry [51]. We note that many details of figure 5, such as the thin-film metallization around the qubit, contacts between chip conductors and antenna and cavity metal, the shape of the antennas and the exact geometry of the cavities, should be optimized by detailed simulation. One comment on the cavity structure: while the cubical cavity satisfies the requirement of three closely spaced modes in an elegant way, it will be perhaps discouragingly large (centimeter-scale) from the point of view of potential scale-up of the surface code. Work is commencing on much different forms of resonator geometries, which by being 'quasi-lumped' [52], can be much more physically compact. It will not be necessary to remain only with the platonic cavities.

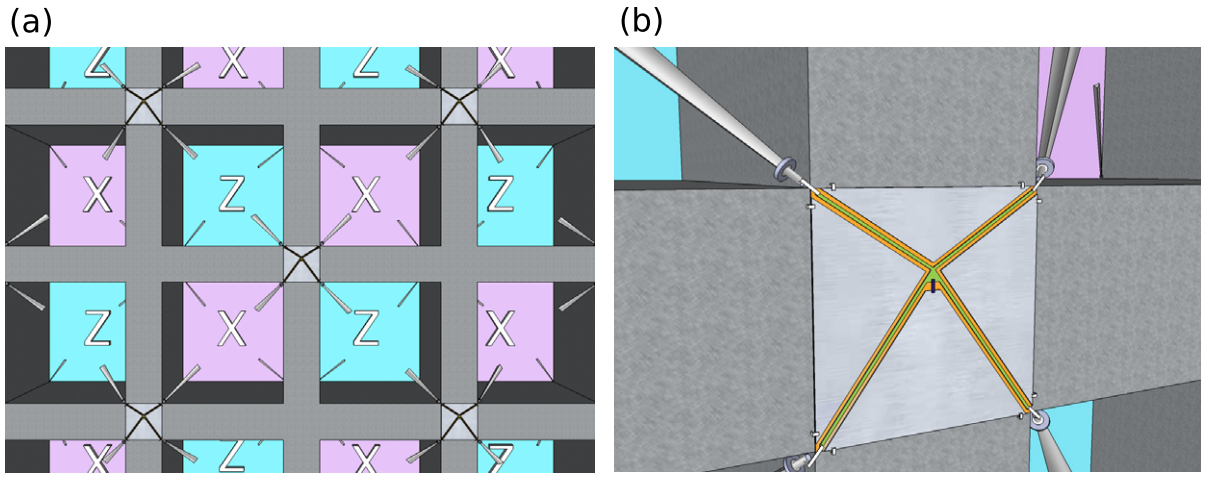

Figure 5. Potentially scalable implementation of the surface code using direct four-qubit parity measurements. (a) Overview of the proposed structure. A solid plate of metal (Al or Cu, as in recent experiments [36, 50]) is perforated with nearly square holes. The thickness of the plate is close to the dimension of the square. When closed with thin top and bottom plates (not shown), these holes become nearly cubical microwave cavities. Qubit structures are grown on chips (lighter squares) using existing thin-film techniques. The insulating side of the chip is mounted to a junction point in the perforated plate; half of the junctions contain chips at the front surface of the plate, and the other half are on the back side (not visible). Each qubit is in electrical contact, via leads going to the corners of the chip, with four antenna structures (tapered rods) projecting diagonally into the four cubical cavities surrounding the chip. Each cavity will enable a four-qubit parity measurement, either ZZZZ or XXXX, as indicated. The external feed lines needed to interrogate each cavity by reflectometry will enter via one of the unoccupied corners of the cubes (not shown). (b) Close-up around one-qubit chip. It could be made in the conventional way, in which a thin film of metal is etched away in slot regions, exposing the underlying insulating substrate (orange). This forms four short segments of coplanar waveguide structures, with the center conductor (green) going to each of the corners of the chip. One small structure (blue) containing a Josephson junction connects the central region of center conductor to one of the ground planes (light gray). The four triangular ground-plane regions are tied to the metal plate, and therefore to each other, by bridges or wire bonds near the corners of the chips. Such bridge/bond connections are also made between the four center conductors and the antenna rods. Insulating support structures isolating the antennas from the conducting walls are only schematically shown. The consequence of this connection arrangement is that the Josephson junction is shunted by four capacitances in series, each formed by an antenna and the side walls of the cavity containing it. Presumed optimal dimensions for the chip (sub-millimeter) and cavity (few centimeter) are not accurately depicted. This figure contains views from a Google Sketchup rendering.

4. Discussion and conclusions

We consider our basic schemes of figures 1 and 5 to be realistic for implementation by experiment. For figure 1, a precise thin-film layout of an on-chip structure (to the right of point P in figure 1) could be devised based on the parameter values we have determined. It is clear that detailed electromagnetic modeling would be useful to guide the layout design [53]. The values obtained for C_a and C_b correspond to well-known few-finger interdigitated capacitors. We foresee three main difficulties: (i) coupling each qubit to the two resonators and (ii) tuning the qubits to achieve the equal-χ condition. The topology of the chip layout would preclude bringing flux-bias lines to each qubit; it is possible that only two of the three qubits would need to be tuned, and one of these tunings could be from an external magnetic field; (iii) measuring few-photon signal levels. It appears that the standard high electron mobility transistor amplifier arrangements would have too much noise for the conditions we have calculated; adoption of new, quantum-limited amplification will be needed for high-fidelity readout.

The 3D scheme of figure 5 will require more work to assess its optimal implementation. Achieving the parameter values envisioned by our theory will require detailed simulation of the complex structure that we have proposed, with many details subject to variation. Since the direct, ancillaless approach studies here are so different from the existing technique of collecting error syndromes with the action of a quantum circuit using ancillas, we believe that it is impossible to know which approach will be superior. Further studies and refinement of both approaches will be necessary to determine which will provide the best way forward.

So, it may be that our proposals can only attain satisfactory performance in structures in which the resonators are tuneable (as in [54–56]), or qubits are tuneable in frequency (as in [15] and in many other works) or in effective coupling strength (as in [57]). Application of these device construction techniques, as well as near-quantum-limited amplification [41], will be likely needed to achieve high-fidelity, single-shot parity measurement as envisioned in the proposals we give here. We hope that following this route will indeed be facilitated by the many interesting experimental [58–60] and theoretical [12, 61, 62] innovations in the application of circuit QED that we see presently.

The proposals of this paper are not the blueprint for a scalable quantum computer; they are concepts on which further detailed studies to determine optimal device functionality can be based. While the structures that we suggest here will by no means be trivially realized, we believe that the crucial role played by parity measurement in the implementation of reliable quantum computation makes these approaches worthwhile to pursue.

Acknowledgments

Thanks to Barbara Terhal for emphasizing the importance of multi-qubit parity measurements for fault-tolerant quantum computation; we thank Jay Gambetta, John Smolin and especially Bob W Newcomb, for ongoing discussions. We are grateful for support from the Alexander von Humboldt foundation.

Appendix

In this appendix, we will compute fidelities between output signals for the case of a finite bandwidth probe.

We compute the fidelity between output signals corresponding to two different qubit states $|\mathbf{s}\rangle$ and $|\mathbf{s}'\rangle$. We first construct the creation operator $\hat{a}^{\dagger}_{\text{pulse}}$ corresponding to a finite bandwidth probe pulse as a linear combination of a densely spaced, discrete set of harmonic modes $\hat{a}^{\dagger}_{\omega_i}$ [63]:

$$\hat{a}^{\dagger}_{\text{pulse}} = \sum_i C_i \hat{a}^{\dagger}_{\omega_i} \tag{A.1}$$

with

$$C_i = \frac{\sqrt{\delta\omega}\mathrm{e}^{-(\omega_i-\omega_\mathrm{p})^2/4W^2}}{\left(2\pi W^2\right)^{1/4}}, \tag{A.2}$$

where ω_p is the center frequency, W is the bandwidth of the probe signal, ω_i is the frequency of mode i and $\delta\omega$ is the difference between frequencies of successive modes. In the above expression, the weight C_i of each term is chosen such that in the limit of a continuum of modes ($\delta\omega \to 0$) the unitarity constraint is satisfied [63]:

$$\sum |C_i|^2 \approx \frac{1}{\sqrt{2\pi W^2}} \int_{-\infty}^{\infty} \mathrm{d}\omega\, \mathrm{e}^{-(\omega-\omega_\mathrm{p})^2/2W^2} \tag{A.3}$$

$$= 1 + O(\delta\omega). \tag{A.4}$$

Now we define a coherent state of amplitude α for probe pulse:

$$|\alpha\rangle = \mathrm{e}^{-|\alpha|^2/2}\, \mathrm{e}^{\alpha \hat{a}^{\dagger}_{\text{pulse}}} |0\rangle\,. \tag{A.5}$$

If we define an amplitude α_i for mode i as follows:

$$\alpha_i \equiv \alpha C_i = \alpha \frac{\sqrt{\delta\omega}\, \mathrm{e}^{-(\omega_i-\omega_\mathrm{p})^2/4W^2}}{\left(2\pi W^2\right)^{1/4}} \tag{A.6}$$

using the fact

$$\lim_{\delta\omega\to 0} \sum_i |\alpha_i|^2 = |\alpha|^2 \lim_{\delta\omega\to 0} \sum_i |C_i|^2 = |\alpha|^2\,, \tag{A.7}$$

we can rewrite the coherent probe state $|\alpha\rangle$ in equation (A.5) in the continuum modes limit as

$$|\alpha\rangle = \mathrm{e}^{-|\alpha|^2/2}\, \mathrm{e}^{\alpha \hat{a}^{\dagger}_{\text{pulse}}} |0\rangle \tag{A.8}$$

$$= \mathrm{e}^{-\frac{1}{2}\sum_i |\alpha_i|^2}\, \mathrm{e}^{\alpha \sum_i C_i \hat{a}^{\dagger}_{\omega_i}} |0\rangle \tag{A.9}$$

$$= \prod_i \mathrm{e}^{-|\alpha_i|^2/2}\, \mathrm{e}^{\alpha_i \hat{a}^{\dagger}_{\omega_i}} |0\rangle \tag{A.10}$$

$$= \prod_i |\alpha_i\rangle\,, \tag{A.11}$$

where we have defined a coherent state for each mode i as

$$|\alpha_i\rangle = \mathrm{e}^{-|\alpha_i|^2/2}\, \mathrm{e}^{\alpha_i \hat{a}^{\dagger}_{\omega_i}} |0\rangle\,. \tag{A.12}$$

Now if the qubits are in state $|\mathbf{s}\rangle$ the coherent component $|\alpha_i\rangle$ of the input probe at frequency ω_i will get a phase shift of $\theta_{\mathbf{s}}(\omega_i)$ and go to the state $\left|\alpha_i\, \mathrm{e}^{\mathrm{i}\theta_{\mathbf{s}}(\omega_i)}\right\rangle$. If we call $|\beta_{\mathbf{s}}\rangle$ the state of the output signal when qubits are in state $|\mathbf{s}\rangle$ we can compute the fidelity

$$\mathcal{F} = \langle \beta_{\mathbf{s}} | \beta_{\mathbf{s}'} \rangle \tag{A.13}$$

$$= \prod_i \left\langle \alpha_i\, \mathrm{e}^{\mathrm{i}\theta_{\mathbf{s}}(\omega_i)} | \alpha_i\, \mathrm{e}^{\mathrm{i}\theta_{\mathbf{s}'}(\omega_i)} \right\rangle \tag{A.14}$$

$$= \prod_i \exp\left\{ - |\alpha_i|^2 \left(1 - \mathrm{e}^{-\mathrm{i}\left(\theta_{\mathbf{s}}(\omega_i) - \theta_{\mathbf{s}'}(\omega_i)\right)}\right)\right\} \tag{A.15}$$

$$= \exp\left\{ - \sum_i |\alpha_i|^2 \left(1 - \mathrm{e}^{-\mathrm{i}\left(\theta_{\mathbf{s}}(\omega_i) - \theta_{\mathbf{s}'}(\omega_i)\right)}\right)\right\}. \tag{A.16}$$

Expanding the phases around the center frequency of the probe $\omega_i = \omega_{\mathrm{p}} + \Delta\omega_i$:

$$\theta_{\mathbf{s}}(\omega_i) = \theta_{\mathbf{s}}\left(\omega_{\mathrm{p}}\right) + \theta'_{\mathbf{s}}\left(\omega_{\mathrm{p}}\right) \Delta\omega_i + O\left((\Delta\omega_i)^2\right), \tag{A.17}$$

$$\theta_{\mathbf{s}'}(\omega_i) = \theta_{\mathbf{s}'}\left(\omega_{\mathrm{p}}\right) + \theta'_{\mathbf{s}'}\left(\omega_{\mathrm{p}}\right) \Delta\omega_i + O\left((\Delta\omega_i)^2\right). \tag{A.18}$$

Now, we consider the case when $\mathbf{s}$ and $\mathbf{s}'$ have the same parity. Then $\theta_{\mathbf{s}}(\omega_{\mathrm{p}}) = \theta_{\mathbf{s}'}(\omega_{\mathrm{p}}) \bmod(2\pi)$, and we get to the first order in $\Delta\omega_i$

$$\mathcal{F} = \exp\left\{ - \sum_i |\alpha_i|^2 \left(1 - \mathrm{e}^{-\mathrm{i}b\Delta\omega_i}\right)\right\}, \tag{A.19}$$

where we have defined

$$b \equiv \theta'_{\mathbf{s}}\left(\omega_{\mathrm{p}}\right) - \theta'_{\mathbf{s}'}\left(\omega_{\mathrm{p}}\right). \tag{A.20}$$

Using the expression for α_i in equation (A.6) and taking the limit of continuum of modes the sum in the exponent of the above expression becomes an integral

$$\mathcal{F} = \exp\left\{ - \frac{|\alpha|^2}{\sqrt{2\pi W^2}} \int_{-\infty}^{\infty} \mathrm{d}\omega\, \mathrm{e}^{-\left(\omega - \omega_{\mathrm{p}}\right)^2 / 2W^2} \left(1 - \mathrm{e}^{-\mathrm{i}b\left(\omega - \omega_{\mathrm{p}}\right)}\right)\right\} \tag{A.21}$$

$$= \exp\left\{ - |\alpha|^2 \left(1 - \mathrm{e}^{-b^2 W^2/2}\right)\right\}. \tag{A.22}$$

If $bW \ll 1$ then $1 - \mathrm{e}^{-b^2W^2/2} \simeq \frac{b^2W^2}{2}$ so that

$$\mathcal{F} \simeq \mathrm{e}^{-|\alpha|^2 b^2 W^2/2}. \tag{A.23}$$

If we further assume that $|\alpha|\, bW \ll 1$ we obtain

$$\mathcal{F} \simeq 1 - \frac{|\alpha|^2\, b^2 W^2}{2}. \tag{A.24}$$

The fidelity between odd and even states is given by a simpler calculation

$$\mathcal{F}_{\mathrm{even/odd}} = \left\langle \alpha\, \mathrm{e}^{\mathrm{i}\theta_{\mathrm{even}}} | \alpha\, \mathrm{e}^{\mathrm{i}\theta_{\mathrm{odd}}} \right\rangle \tag{A.25}$$

$$= \mathrm{e}^{-|\alpha|^2(1 - \cos\Delta\theta)} \approx \mathrm{e}^{-2|\alpha|^2}. \tag{A.26}$$

The final expression is a consequence of the fact that $\Delta\theta \approx \pi$.

Another case we look at, relevant for the alternative scheme of [8], is the case of matching linear dispersion (i.e. $b = 0$) but finite quadratic dispersion mismatch

$$b' \equiv \left.\frac{\mathrm{d}^2\theta_{\mathrm{s}}(\omega)}{\mathrm{d}\omega^2}\right|_{\omega_{\mathrm{p}}} - \left.\frac{\mathrm{d}^2\theta_{\mathrm{s}}(\omega)}{\mathrm{d}\omega^2}\right|_{\omega_{\mathrm{p}}}. \tag{A.27}$$

Then the fidelity, for the case of the same parity, is

$$\mathcal{F} = \left|\exp\left\{-\sum_i |\alpha_i|^2 \left(1 - \mathrm{e}^{-\mathrm{i}b'(\Delta\omega_i)^2}\right)\right\}\right|. \tag{A.28}$$

Again in the limit of continuum of modes $\mathcal{F}$ becomes

$$\mathcal{F} = \left|\exp\left\{-\frac{|\alpha|^2}{\sqrt{2\pi W^2}}\int_{-\infty}^{\infty} \mathrm{d}\omega\, \mathrm{e}^{-(\omega-\omega_{\mathrm{p}})^2/2W^2}\left(1 - \mathrm{e}^{-\mathrm{i}b'(\omega_i-\omega_{\mathrm{p}})^2}\right)\right\}\right| \tag{A.29}$$

$$= \left|\exp\left\{-|\alpha|^2\left(1 - \frac{1}{\sqrt{1+2\mathrm{i}b'W^2}}\right)\right\}\right| \tag{A.30}$$

$$= \exp\left\{Re\left[-|\alpha|^2\left(1 - \frac{1}{\sqrt{1+2\mathrm{i}b'W^2}}\right)\right]\right\} \tag{A.31}$$

$$= \exp\left\{-|\alpha|^2\left(1 - \sqrt{\frac{1+\sqrt{1+4b'^2W^4}}{2+8b'^2W^4}}\right)\right\} \tag{A.32}$$

$$\simeq 1 - \frac{3|\alpha|^2 b'^2 W^4}{2} + O\left(|\alpha|^4\left(b'W^2\right)^4\right), \tag{A.33}$$

where we assumed that $b'W^2 \ll 1$ and $|\alpha|\, b'W^2 \ll 1$.

To obtain an estimate for the power of the measurement signal, we assume that the signal contains $|\alpha|^2 = 5$ photons and that it has duration $T = 1\,\mu$s so that the peak power P will roughly be $P = \frac{|\alpha|^2\hbar\omega_{\mathrm{p}}}{T} = -135\,\mathrm{dBm}$.

References

[1] Mermin N D 2007 *Quantum Computer Science: An Introduction* (Cambridge: Cambridge University Press)

[2] Dennis E, Kitaev A, Landahl A and Preskill J 2002 Topological quantum memory *J. Math. Phys.* **43** 4452–505

[3] Scully M O and Druhl K 1982 Quantum eraser: a proposed photon correlation experiment concerning observation and 'delayed choice' in quantum mechanics *Phys. Rev.* A **25** 2208–13

[4] Gottesman D 1999 Fault-tolerant quantum computation with higher-dimensional systems *Chaos Solitons Fractals* **10** 1749–58

[5] Beenakker C W J, DiVincenzo D P, Emary C and Kindermann M 2004 Charge detection enables free-electron quantum computation *Phys. Rev. Lett.* **93** 020501

[6] Engel H-A and Loss D 2005 Fermionic Bell-state analyzer for spin qubits *Science* **309** 586–8

[7] Trauzettel B, Jordan A N, Beenakker C W J and Buttiker M 2006 Parity meter for charge qubits: an efficient quantum entangler *Phys. Rev.* B **73** 235331

[8] Kerckhoff J, Bouten L, Silberfarb A and Mabuchi H 2009 Physical model of continuous two-qubit parity measurement in a cavity-QED network *Phys. Rev.* A **79** 024305

[9] Lalumiere K, Gambetta J M and Blais A 2010 Tunable joint measurements in the dispersive regime of cavity QED *Phys. Rev.* A **81** 040301
[10] Tornberg L and Johansson G 2010 High-fidelity feedback-assisted parity measurement in circuit QED *Phys. Rev.* A **82** 012329
[11] Mao W, Averin D V, Ruskov R and Korotkov A N 2004 Mesoscopic quadratic quantum measurements *Phys. Rev. Lett.* **93** 056803
[12] Feng W, Wang P, Ding X, Xu L and Li X-Q 2011 Generating and stabilizing the GHZ state in circuit QED: joint measurement, Zeno effect and feedback *Phys. Rev.* A **83** 042313
[13] Chow J M, DiCarlo L, Gambetta J M, Nunnenkamp A, Bishop L S, Frunzio L, Devoret M H, Girvin S M and Schoelkopf R J 2010 Entanglement metrology using a joint readout of superconducting qubits *Phys. Rev.* A **81** 062325
[14] Filipp S *et al* 2009 Two-qubit state tomography using a joint dispersive read-out *Phys. Rev. Lett.* **102** 200402
[15] DiCarlo L *et al* 2009 Demonstration of two-qubit algorithms with a superconducting quantum processor *Nature* **460** 240–4
[16] Ristè D, van Leeuwen J G, Ku H-S, Lehnert K W and DiCarlo L 2012 Initialization by measurement of a two-qubit superconducting circuit *Phys. Rev. Lett.* **109** 050507
[17] Devitt S J, Munro W J and Nemoto K 2013 Quantum error correction for beginners *Rep. Prog. Phys.* at press (arXiv:0905.2794v3)
[18] Denhez G, Blais A and Poulin D 2012 Quantum error correction benchmarks for continuous weak parity measurements *Phys. Rev.* A **86** 032318
[19] Suchara M, Bravyi S and Terhal B M 2011 Constructions and noise threshold of topological subsystem codes *Phys. J.* A **44** 155301
[20] Raussendorf R and Harrington J 2007 Fault-tolerant quantum computation with high threshold in two dimensions *Phys. Rev. Lett.* **98** 190504
[21] Bacon D 2006 Operator quantum error correcting subsystems for self-correcting quantum memories *Phys. Rev.* A **73** 012340
[22] Aliferis P and Cross A W 2007 Subsystem fault tolerance with the Bacon–Shor code *Phys. Rev. Lett.* **98** 220502
[23] Cross A W, DiVincenzo D P and Terhal B M 2009 A comparative code study for quantum fault-tolerance *Quantum Inform. Comput.* **9** 0541–72
[24] DiVincenzo D P 2009 Fault tolerant architectures for superconducting qubits *Phys. Scr.* **T137** 014020
[25] Fowler A G, Stephens A M and Groszkowski P 2009 High threshold universal quantum computation on the surface code *Phys. Rev.* A **80** 052312
[26] Horsman C, Fowler A G, Devitt S and Van Meter R 2012 Surface code quantum computing by lattice surgery *New J. Phys.* **14** 123011
[27] Bravyi S, Duclos-Cianci G, Poulin D and Suchara M 2012 Subsystem surface codes with three-qubit check operators arXiv:1207.1443
[28] Yamaguchi F, Nemoto K and Munro W J 2006 Quantum error correction via robust probe modes *Phys. Rev.* A **73** 060302
[29] Nigg S E and Girvin S M 2012 Stabilizer quantum error correction toolbox for superconducting qubits arXiv:1212.4000v2
[30] Koch J, Yu T M, Gambetta J, Houck A A, Schuster D I, Majer J, Blais A, Devoret M H, Girvin S M and Schoelkopf R J 2007 Charge insensitive qubit design derived from the Cooper pair box *Phys. Rev.* A **76** 042319
[31] Steffen M, Kumar S, DiVincenzo D P, Rozen J R, Keefe G A, Rothwell M B and Ketchen M B 2010 High-coherence hybrid superconducting qubit *Phys. Rev. Lett.* **105** 100502
[32] Blais A, Gambetta J, Wallraff A, Schuster D I, Girvin S M, Devoret M H and Schoelkopf R J 2007 Quantum information processing with circuit quantum electrodynamics *Phys. Rev.* A **75** 032329
[33] Blais A, Huang R-S, Wallraff A, Girvin S M and Schoelkopf R J 2004 Cavity quantum electrodynamics for superconducting electrical circuits: an architecture for quantum computation *Phys. Rev.* A **69** 062320

[34] Johnson B R *et al* 2010 Quantum non-demolition detection of single microwave photons in a circuit *Nature Phys.* **6** 663–7
[35] Mariantoni M *et al* 2011 Implementing the quantum von Neumann architecture with superconducting circuits *Science* **334** 61–5
[36] Paik H *et al* 2011 Observation of high coherence in Josephson junction qubits measured in a three-dimensional circuit QED architecture *Phys. Rev. Lett.* **107** 240501
[37] Ramo S, Whinnery J R and van Duzer T 1965 *Fields and Waves in Communication Electronics* (New York: Whiley) chapter 10.07
[38] Pozar D 2005 *Microwave Engineering* 3rd edn (New York: Wiley)
[39] Goppl M, Fragner A, Baur M, Bianchetti R, Filipp S, Fink J M, Leek P J, Puebla G, Steffen L and Wallraff A 2008 Coplanar waveguide resonators for circuit quantum electrodynamics *J. Appl. Phys.* **104** 113904
[40] Walls D F and Milburn G J 2008 *Quantum Optics* 2nd edn (Berlin: Springer)
[41] Vijay R, Slichter D H and Siddiqi I 2011 Observation of quantum jumps in a superconducting artificial atom *Phys. Rev. Lett.* **106** 110502
[42] Newcomb R W 1966 *Linear Multiport Synthesis* (New York: McGraw-Hill) chapter 3
[43] Bergeal N, Vijay R, Manucharyan V E, Siddiqi I, Schoelkopf R J, Girvin S M and Devoret M H 2010 Analog information processing at the quantum limit with a Josephson ring modulator *Nature Phys.* **6** 296–302
[44] Koch J, Houck A A, Le Hur K and Girvin S M 2010 Time-reversal symmetry breaking in circuit-QED based photon lattices *Phys. Rev.* A **82** 043811
[45] Simons R N 2001 *Coplanar Waveguide Circuits, Components and Systems* (*Wiley Series in Microwave and Optical Engineering*) (New York: Wiley)
[46] Ku H S, Mallet F, Vale L R, Irwin K D, Russek S E, Hilton G C and Lehnert K W 2011 Design and testing of superconducting microwave passive components for quantum information processing *IEEE. Trans. Appl. Supercond.* **21** 452–5
[47] Poletto S *et al* 2012 Entanglement of two superconducting qubits in a waveguide cavity via monochromatic two-photon excitation *Phys. Rev. Lett.* **109** 240505
[48] Gambetta J M 2012 private communication
[49] Fowler A G, Mariantoni M, Martinis J M and Cleland A N 2012 Surface codes: towards practical large-scale quantum computation *Phys. Rev.* A **86** 032324
[50] Rigetti C *et al* 2012 Superconducting qubit in waveguide cavity with coherence time approaching 0.1 ms *Phys. Rev.* B **86** 100506
[51] Nigg S E, Paik H, Vlastakis B, Kirchmair G, Shankar S, Frunzio L, Devoret M, Schoelkopf R and Girvin S 2012 Black-box superconducting circuit quantization *Phys. Rev. Lett.* **108** 240502
[52] Khalil M S, Wellstood F C and Osborn K D 2011 Loss dependence on geometry and applied power in superconducting coplanar resonators *IEEE Trans. Appl. Supercond.* **21** 879–82
[53] Watson P M and Gupta K C 1997 Design and optimization of CPW circuits using EM-ANN models for CPW components *IEEE Trans. Micro. Theory Technol.* **45** 2515–23
[54] Wilson C M, Persson F, Bauch T, Johansson G, Shumeiko V, Duty T and Delsing P 2008 Tuning the field in a microwave resonator faster than the photon lifetime *Appl. Phys. Lett.* **92** 203501
[55] Ong F R, Boissonneault M, Mallet F, Palacios-Laloy A, Dewes A, Doherty A C, Blais A, Bertet P, Vion D and Esteve D 2011 Circuit QED with a nonlinear resonator: ac-stark shift and dephasing *Phys. Rev. Lett.* **106** 167002
[56] Castellanos-Beltran M A, Irwin K D, Hilton G C, Vale L R and Lehnert K W 2008 Amplification and squeezing of quantum noise with a tunable Josephson metamaterial *Nature Phys.* **4** 929
[57] Gambetta J M, Houck A A and Blais A 2011 A superconducting qubit with Purcell protection and tunable coupling *Phys. Rev. Lett.* **106** 030502
[58] Mariantoni M, Menzel E P, Deppe F, Araque Caballero M A, Baust A, Niemczyk T, Hoffmann E, Solano E, Marx A and Gross R 2010 Planck spectroscopy and the quantum noise of microwave beam splitters *Phys. Rev. Lett.* **105** 133601

[59] Reuther G M *et al* 2010 Two-resonator circuit QED: dissipative theory *Phys. Rev.* B **81** 144510
[60] Hoi I-C, Wilson C M, Johansson G, Palomaki T, Peropadre B and Delsing P 2011 Demonstration of a single-photon router in the microwave regime *Phys. Rev. Lett.* **107** 073601
[61] Chirolli L, Burkard G, Kumar S and DiVincenzo D P 2010 Superconducting resonators as beam splitters for linear-optics quantum computation *Phys. Rev. Lett.* **104** 230502
[62] Shen J T and Fan S 2005 Coherent single photon transport in a one-dimensional waveguide coupled with superconducting quantum bits *Phys. Rev. Lett.* **95** 213001
[63] Titulaer U M and Glauber R J 1966 Density operators for coherent fields *Phys. Rev.* **145** 1041–50